

# Synthesis of {110}-Faceted Gold Bipyramids and Rhombic Dodecahedra

Michelle L. Personick, Mark R. Langille, Jian Zhang, Nadine Harris, George C. Schatz, and Chad A. Mirkin\*

Department of Chemistry and International Institute for Nanotechnology, Northwestern University,  
2145 Sheridan Road, Evanston, IL 60208

E-mail: chadnano@northwestern.edu

## Experimental Details

**Chemicals.** Gold (III) chloride trihydrate ( $\text{HAuCl}_4 \cdot 3\text{H}_2\text{O}$ , 99.9+%), silver nitrate ( $\text{AgNO}_3$ , 99.9999%), sodium borohydride ( $\text{NaBH}_4$ , 99.99%), sodium chloride ( $\text{NaCl}$ , 99.999%), L-ascorbic acid (AA, 99+%), and cetyltrimethylammonium chloride (CTAC, 25 wt.% in  $\text{H}_2\text{O}$ ) were purchased from Aldrich and used without further purification. Hydrochloric acid ( $\text{HCl}$ , 1 mol/L volumetric solution) was purchased from Fluka and used without further purification.

**Synthesis of Au Seeds.** Au seeds were prepared by quickly injecting 0.60 mL of ice-cold, freshly prepared  $\text{NaBH}_4$  (10 mM) into a rapidly stirring solution containing 0.25 mL of  $\text{HAuCl}_4$  (10 mM) and 10.00 mL of CTAC (100 mM). The seed solution was stirred for 1 minute and then left undisturbed for 2 hours.

**Synthesis of Single Crystal Seeds.** Single crystal seeds were prepared according to a previously published procedure.<sup>1</sup>

**Synthesis of Rhombic Dodecahedra and Bipyramids.** A growth solution was prepared by consecutively adding 0.50 mL of  $\text{HAuCl}_4$  (10 mM), 0.01 mL of  $\text{AgNO}_3$  (10 mM), 0.20 mL of  $\text{HCl}$  (1.0 M), then 0.10 mL of ascorbic acid (100 mM) into 10.00 mL of 0.04 M CTAC. The seed particles were serially diluted in 0.1 M CTAC to generate a solution which was 1/1000 the concentration of the original seed solution. Particle growth was initiated by adding 0.1 mL of the diluted seeds to the growth solution. The reaction was swirled immediately after the addition of the seeds and then left undisturbed on the bench top until the reaction was complete. Bipyramids were isolated from rhombic dodecahedra via vacuum filtration with a 0.1  $\mu\text{m}$  pore size filter (Whatman Anodisc 47, 0.1  $\mu\text{m}$  pore, 47 mm). Alternatively, rhombic dodecahedra can also be isolated from the combined reaction mixture via syringe filtration using a syringe-driven filter with pore size  $\leq 0.2 \mu\text{m}$  (PALL Life Sciences Acrodisc LC 25 mm syringe filter, 0.2  $\mu\text{m}$  pore PVDF membrane).

**Characterization.** Scanning electron microscopy (SEM) images were obtained using a Hitachi S-4800-II cFEG SEM. Transmission electron microscopy (TEM) images and electron diffraction patterns were obtained using a Hitachi H-8100 TEM and high-resolution TEM (HR-TEM) images were obtained using a JEOL JEM-2100F FEG Fas-TEM. UV-Vis absorption data were obtained using a Cary-5000 UV-Vis spectrophotometer.

**Calculated Spectra.** DDA calculations were performed on a bipyramid (BP) with an effective edge length of  $a = 270 \text{ nm}$  with  $b \sim 156 \text{ nm}$  and  $h \sim 89 \text{ nm}$  calculated from the equations in Figure 1F. Orientationally-averaged calculations were performed where the BP target was assumed to have two unit vectors  $\hat{\mathbf{a}}_1$  and  $\hat{\mathbf{a}}_2$  fixed within the target with  $\hat{\mathbf{a}}_1$  describing the height ( $h$ ) (along the x-axis) of the BP and  $\hat{\mathbf{a}}_2$  orthogonal to  $\hat{\mathbf{a}}_1$ . To perform orientation averaging, the BP target was rotated  $90^\circ$  (in three

incremental steps) through the angles of  $\theta$  and  $\phi$  which specify the direction of  $\hat{\mathbf{a}}_1$  with respect to the incident wavevector  $\mathbf{k}$ . The wavevector was taken to be along the x-axis and polarization along both y- and z-axes was considered. The dielectric table of Frederikse and Weaver<sup>2</sup> for electropolished Au was used and the incident wavelength and the refractive index were divided by the refractive index of water (1.331) to get the relative refractive index. A dipole spacing of 2 nm was used with a spectral resolution of 10 nm.

The normalized calculated BP extinction spectrum (Figure 3B) displays resonance peaks very close to those measured experimentally with UV-Vis spectroscopy with a dipole mode ( $n = 1$ ) evident at  $\sim 1110$  nm, a higher order quadrupole mode ( $n = 2$ ) at  $\sim 750$  nm, and an octopole mode ( $n = 3$ ) at  $\sim 600$  nm. The synthesized BPs have slightly rounded edges and an average size distribution of  $a = 270 \text{ nm} \pm 26 \text{ nm}$ . Neither the rounded edges nor averaging over the size distribution has been considered in the calculated spectrum in Figure 3B. Considering the excellent agreement between calculated and experimental resonant wavelengths this would suggest that there is apparently a cancellation of effects due to edge rounding and size distribution averaging. However averaging over a distribution of edge sizes will broaden and reduce the intensity of the 1110 nm peak in Fig. 3B while not changing the intensity of the 750 nm and 600 nm peaks as higher multipoles are less sensitive to inhomogeneities than is the dipole mode.

Additional calculations (not shown here) with the BP orientation fixed with respect to the incident polarization were performed to provide further insights to the assignment of these modes. The dipole resonance involves polarization that is primarily in the equatorial plane of the BP. The first multipole ( $n = 2$  at  $\sim 750$  nm) is mostly an in-plane quadrupole, while the octopole ( $n = 3$  at  $\sim 600$  nm) is a combination of both the in-plane and out-of-plane excitations. There are small shifts between in-plane and out-of-plane extinction maxima for the octopole and as a result the orientationally-averaged spectrum is broad and not entirely symmetrical.

- (1) Niu, W. X.; Zheng, S. L.; Wang, D. W.; Liu, X. Q.; Li, H. J.; Han, S. A.; Chen, J.; Tang, Z. Y.; Xu, G. B. *J. Am. Chem. Soc.* **2009**, *131*, 697.
- (2) Weaver, J. H.; Frederikse, H. P. R. *Optical properties of selected elements*, 82<sup>nd</sup> ed. CRC Press: Boca Raton, 2001, p 12.

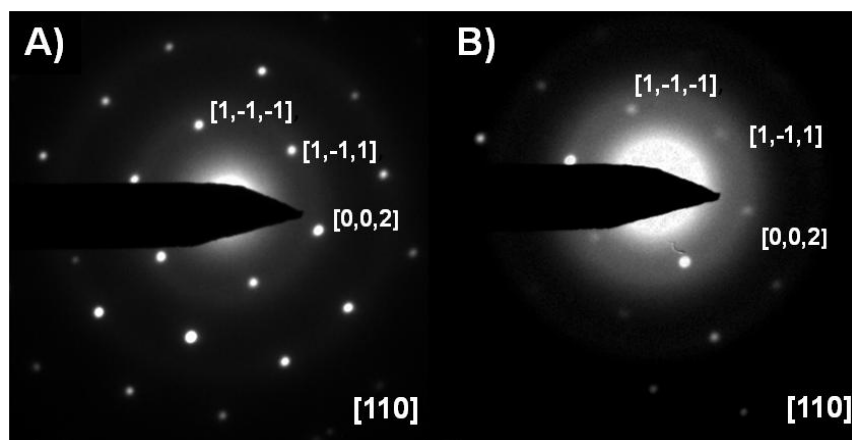


**Figure S1.** Diffraction patterns of (A) bipyramids and (B) rhombic dodecahedra with  $\{110\}$  facet oriented perpendicular to electron beam.

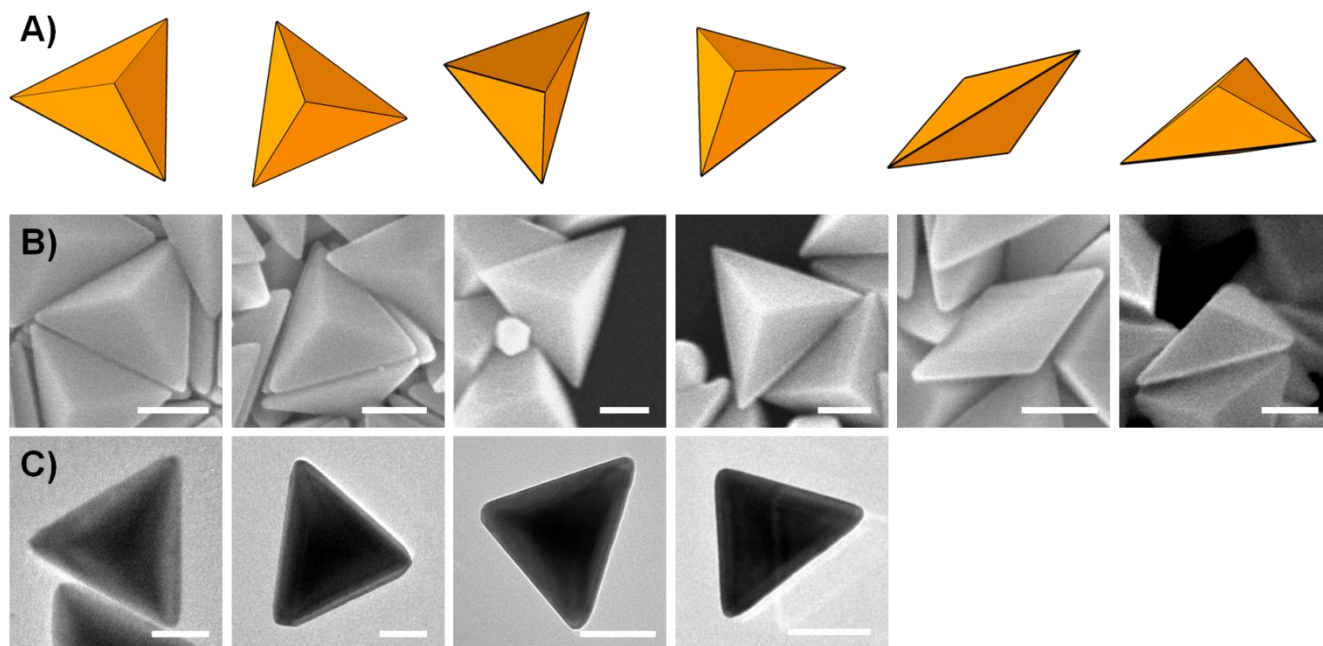


**Figure S2.** (A) Model, (B) high-magnification SEM, and (C) TEM of individual bipyramids in various orientations. Scale bars: 100 nm.

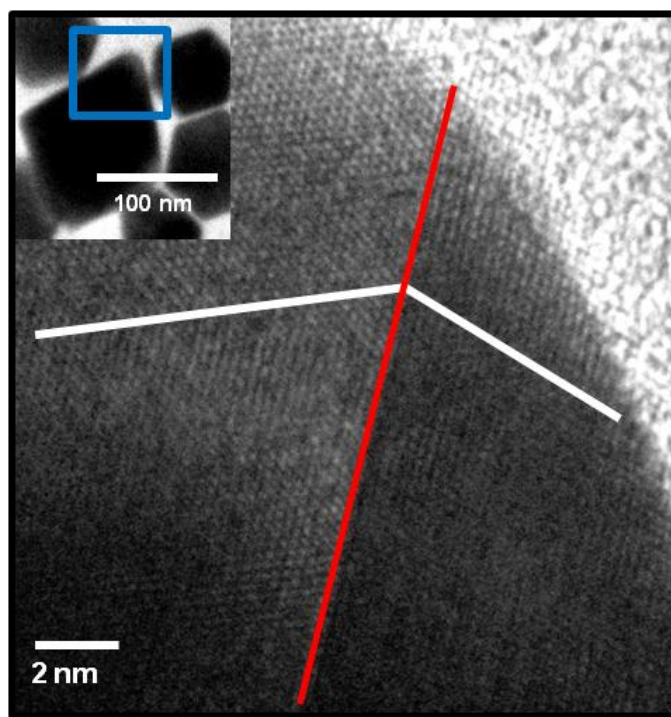


**Figure S3.** HR-TEM image of a single bipyramid (inset) containing a twin plane (red line).

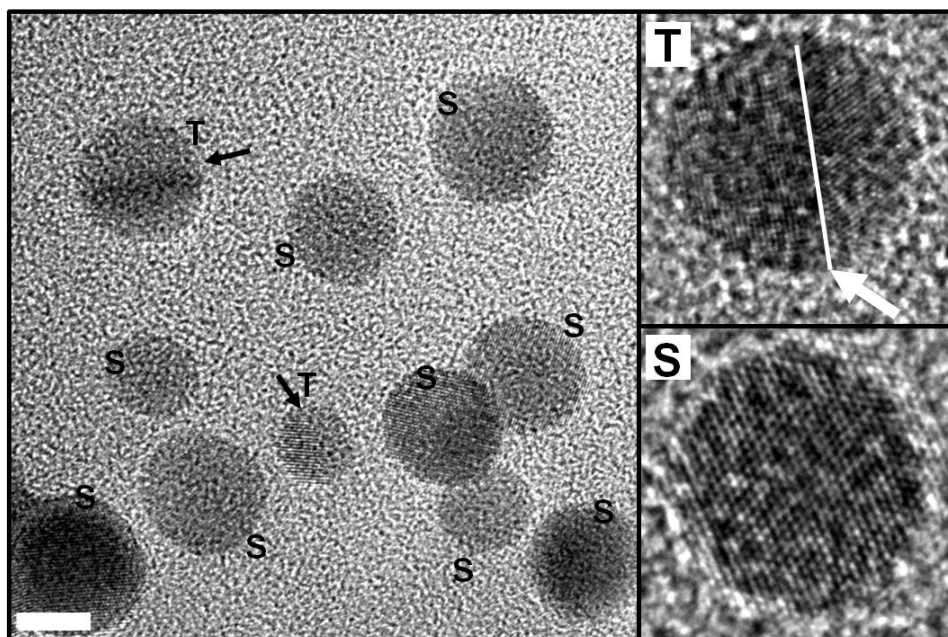


**Figure S4.** Left: HR-TEM of CTAC-stabilized seed particles. Both twinned and single-crystal seeds are observed, indicated by a T or an S, respectively. Arrows indicate twin boundaries. Scale bar: 5 nm. Right: Examples of twinned (top) and single-crystalline (bottom) seed particles.

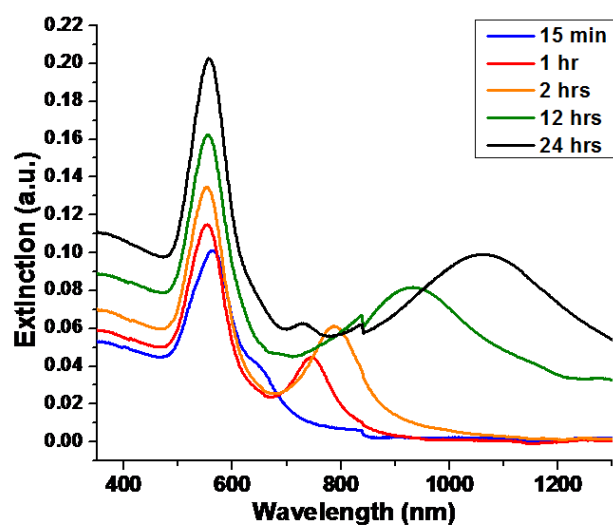


**Figure S5.** Time-dependent UV-vis spectra monitoring the growth of RD and BPs.

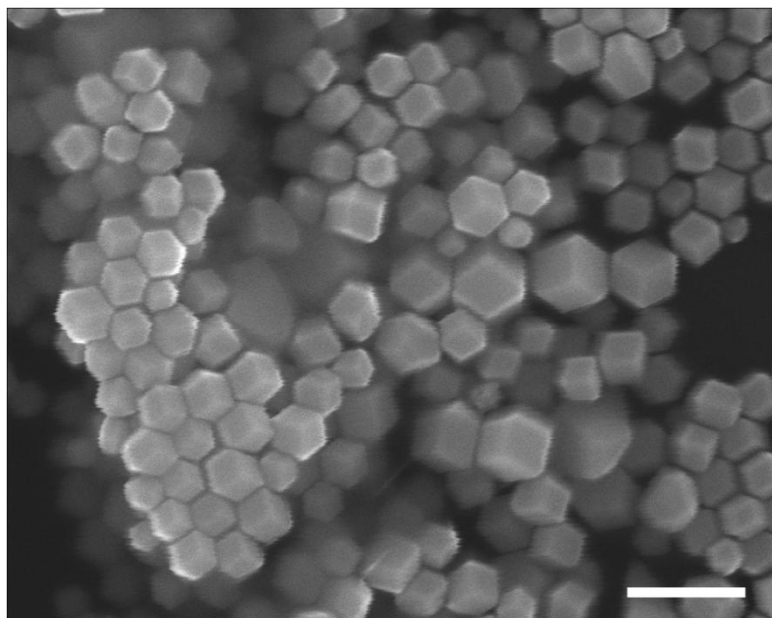


**Figure S6.** SEM of rhombic dodecahedra synthesized with single-crystal seeds. Scale bar: 200 nm.

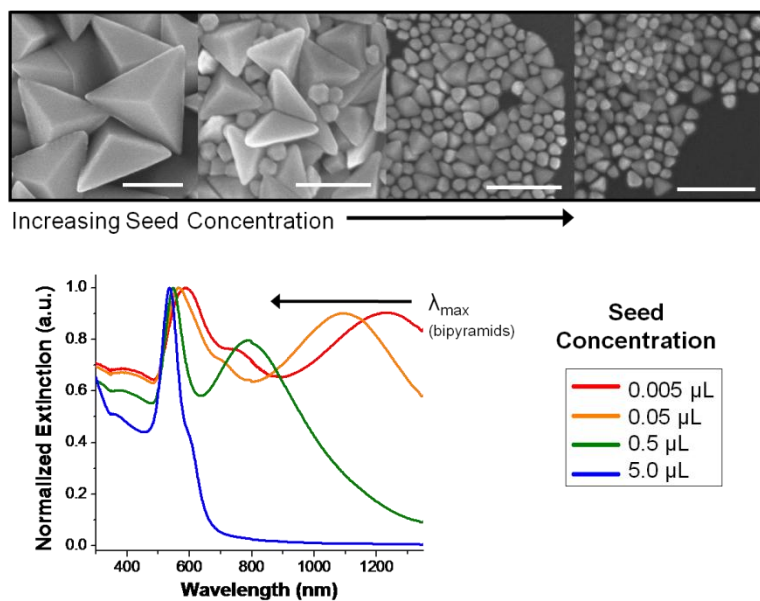


**Figure S7.** Bipyramids and rhombic dodecahedra grown from the addition of (left to right): 0.005  $\mu\text{L}$ , 0.05  $\mu\text{L}$ , 0.5  $\mu\text{L}$ , and 5.0  $\mu\text{L}$  of seed solution. Scale bars: 200 nm. UV-Vis spectra of RD/BP solutions synthesized from increasing amounts of seed particles. Increasing seed concentration results in smaller product particles.

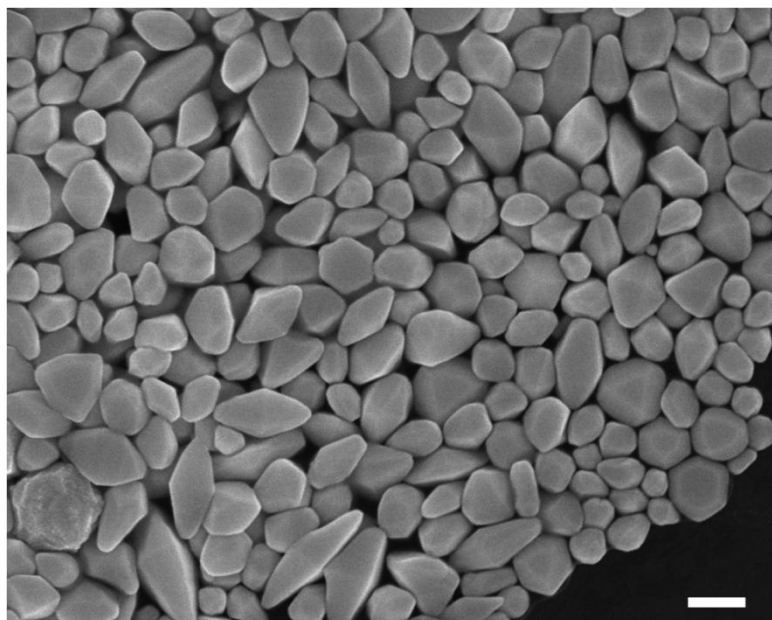


**Figure S8.** SEM of particles synthesized in CTAB with 10  $\mu\text{M}$   $\text{Ag}^+$ . Scale bar: 200 nm.